THE JOURNAL OF BIOLOGICAL CHEMISTRY VOL. 281, NO. 26, pp. 17909–17919, June 30, 2006

Identification of Ligands with Bicyclic Scaffolds Provides Insights into Mechanisms of Estrogen Receptor Subtype Selectivity*[S]

Received for publication, December 22, 2005, and in revised form, April 28, 2006 Published, JBC Papers in Press, April 28, 2006, DOI 10.1074/jbc.M513684200

Robert W. Hsieh[‡§¶1], Shyamala S. Rajan[‡], Sanjay K. Sharma[‡], Yuee Guo[‡], Eugene R. DeSombre[‡], Milan Mrksich[¶2], and Geoffrey L. Greene[‡§3]

From the [‡]Ben May Institute for Cancer Research, the [§]Department of Biochemistry and Molecular Biology, and the [¶]Howard Hughes Medical Institute and Department of Chemistry, University of Chicago, Chicago, Illinois 60637

Estrogen receptors α (ERα) and β (ERβ) have distinct functions and differential expression in certain tissues. These differences have stimulated the search for subtype-selective ligands. Therapeutically, such ligands offer the potential to target specific tissues or pathways regulated by one receptor subtype without affecting the other. As reagents, they can be utilized to probe the physiological functions of the ER subtypes to provide information complementary to that obtained from knock-out animals. A fluorescence resonance energy transfer-based assay was used to screen a 10,000-compound chemical library for ER agonists. From the screen, we identified a family of ERβ-selective agonists whose members contain bulky oxabicyclic scaffolds in place of the planar scaffolds common to most ER ligands. These agonists are 10–50-fold selective for ERβ in competitive binding assays and up to 60-fold selective in transactivation assays. The weak uterotrophic activity of these ligands in immature rats and their ability to stimulate expression of an ERβ regulated gene in human U2OS osteosarcoma cells provides more physiological evidence of their ERβ-selective nature. To provide insight into the molecular mechanisms of their activity and selectivity, we determined the crystal structures of the ERα ligand-binding domain (LBD) and a peptide from the glucocorticoid receptor-interacting protein 1 (GRIP1) coactivator complexed with the ligands OBCP-3M, OBCP-2M, and OBCP-1M. These structures illustrate how the bicyclic scaffolds of these ligands are accommodated in the flexible ligand-binding pocket of ER. A comparison of these structures with existing ER structures suggests that the ERβ selectivity of OBCP ligands can be attributed to a combination of their interactions with Met-336 in ERβ and Met-421 in ERα. These bicyclic ligands show promise as lead compounds that can target ERβ. In addition, our understanding of the molecular determinants of their subtype selectivity provides a useful starting point for developing other ER modulators belonging to this relatively new structural class.

Estrogen receptors α (ERα)[4] and β (ERβ) are ligand-inducible transcription factors that are involved in regulating cell growth, proliferation, and differentiation in various normal and cancerous tissues (1–3). Although the two subtypes of ER bind the endogenous estrogen, 17β-estradiol (E2), with similar affinity (4), they differ in size, share modest sequence identity (47%), and are encoded by different genes (5, 6). Studies of knock-out mice have also shown that the two subtypes have distinct functions and are differentially expressed in certain tissues (1). These differences have stimulated the search for subtype-specific ligands that can elicit tissue- or cell-specific ER activity. In particular, the dominance of ERα expression in the breast and uterus (7) suggests that ERβ-selective ligands may offer some of the benefits of hormone replacement therapy such as a decrease in the risk of colorectal cancer (8) without increasing the risk of breast or uterine cancer. The recent discovery of ERβ-selective ligands that display pathway-specific anti-inflammatory activity without classic estrogenic effects is an example of the possible therapeutic potential of subtype-selective ligands (9). Furthermore, subtype-selective ligands show promise as reagents to probe the physiological functions of ERα and ERβ (10–12), providing complementary information to studies in knock-out mice (1).

Progress towards the development of subtype-selective ligands was significantly advanced with the reports of crystal structures of ERα (13) and ERβ (14). The ligand-binding pockets of the subtypes are similar but not identical. The ERβ ligand-binding pocket is smaller (390 Å^3 *versus* 490 Å^3 for ERα) and differs in two residues from ERα; Leu-384 and Met-421 in ERα are replaced by Met-336 and Ile-373, respectively, in ERβ (14). Notably, these two substitutions give rise to the selectivity of ligands for ERα or ERβ. Although several ERβ-selective ligands have been described (15), only a small number of crystal structures for these ligands complexed with ERβ (14, 16–20) and ERα (17, 20, 21) have been reported. These structures have provided valuable insights into possible molecular mechanisms of ERβ selectivity. However, when one consid-

* This work was supported by the Ludwig Fund for Cancer Research; NCI, National Institutes of Health, Grant CA89489; and Department of Defense Grant W81XWH-04-1-0791. Use of the Argonne National Laboratory Structural Biology Center and BioCARS beamlines at the Advanced Photon Source was supported by the United States Department of Energy, Office of Energy Research, under Contract W-31-109-ENG-38. Use of the BioCARS Sector 14 was also supported by the National Institutes of Health, National Center for Research Resources, under Grant RR07707. The costs of publication of this article were defrayed in part by the payment of page charges. This article must therefore be hereby marked "*advertisement*" in accordance with 18 U.S.C. Section 1734 solely to indicate this fact.

[S] The on-line version of this article (available at http://www.jbc.org) contains supplemental Fig. S1.

The atomic coordinates and structure factors (code 1ZKY, 2FAI, and 2B1V) have been deposited in the Protein Data Bank, Research Collaboratory for Structural Bioinformatics, Rutgers University, New Brunswick, NJ (http://www.rcsb.org/).

[1] Supported by the University of Chicago unendowed Medical Scientist Training Program.

[2] To whom correspondence may be addressed: Dept. of Chemistry and Howard Hughes Medical Institute, University of Chicago, 929 E. 57th St., Chicago, IL 60637. Tel.: 773-702-1651; Fax: 773-702-1677; E-mail: mmrksich@uchicago.edu.

[3] To whom correspondence may be addressed: Ben May Institute for Cancer Research, University of Chicago, W330, 929 E. 57th St., Chicago, IL 60637. Tel.: 773-702-6964; Fax: 773-834-9029; E-mail: ggreene@uchicago.edu.

[4] The abbreviations used are: ER, estrogen receptor; hER, human ER; E2, 17β-estradiol; SAR, structure-activity relationship; LBD, ligand-binding domain; GRIP1, glucorticoid receptor-interacting protein 1; DPN, diarylpropionitrile; PPT, propylpyrazole triol; SRC1, steroid receptor coactivator 1; GST, glutathione *S*-transferase; β-ME, β-mercaptoethanol; OBCP-*x*M, oxabicyclic phenol with *x* methyls on the core scaffold; HTRF, homogenous time-resolved fluorescence; AR, androgen receptor; NRD, nuclear receptor interaction domain; ERE, estrogen response element; ARE, androgen response element; DES, diethlystilbestrol; MonA, monomer A; MonB, monomer B.

ers the structural diversity of the known ERβ-selective ligands and the plasticity of the ER ligand-binding pocket, it is clear that more structures of ER subtype-selective ligands are needed to develop general mechanisms for subtype selectivity.

We describe here the identification and characterization of a family of ligands sharing an oxabicyclic scaffold that are ER agonists and variably selective for ERβ. These ligands possess bulky bicyclic scaffolds that differ from the planar scaffolds common to most estrogenic compounds. Cell and animal studies demonstrate the promise of these ligands as agents that can target ERβ for therapeutic or investigational purposes. In addition, we obtained crystal structures with three of these ligands, OBCP-3M, OBCP-2M, and OBCP-1M, in complex with the ERα ligand-binding domain (LBD) and a glucocorticoid receptor-interacting protein 1 (GRIP1) peptide. These structures provide evidence to suggest that the ERβ selectivity of the OBCP ligands can be attributed to their interactions with only two residues: Met-336 in ERβ and Met-421 in ERα.

EXPERIMENTAL PROCEDURES

Reagents—The 10,000-compound chemical library (Library ET 350-1) used for ligand screening was obtained from ChemBridge (San Diego, CA). The means and S.D. values of clogP and molecular weight values for this library are 3.7 ± 1.6 and 340 ± 71, respectively. All compounds from the 5474 family (except OBCP-2M) were also obtained from ChemBridge. OBCP-2M was synthesized according to reported procedures for analogous compounds (23, 24). E2 and genistein were obtained from Sigma. Diarylpropionitrile (DPN) and propylpyrazole triol (PPT) were obtained from Tocris Bioscience (Ellisville, MO). [^{3}H]E2 was obtained from American Radiolabeled Chemicals (St. Louis, MO).

Plasmids—Many of the plasmids used in these studies were generous gifts from colleagues: pGST-ERα-LBD (ERα residues 282–595) from Dr. Peter Kushner (University of California, San Francisco, CA), pCR3.1.SRC1 from Dr. Ming-Jer Tsai and Dr. Sophia Y. Tsai (Baylor College of Medicine, Houston, TX), p3×ERE-Luc from Dr. Donald McDonnell (Duke University, Durham, NC), pCMV5-hERβ (full-length ERβ) and p6×His-ERβ LBD (residues 256–505) from Dr. Benita Katzenellenbogen (University of Illinois, Champaign, IL), HEGO/pSG5 (full-length ERα) from Dr. Pierre Chambon (Institute of Genetics and Molecular and Cellular Biology, Strasbourg, France), pAR and p3×ARE-Luc from Dr. Shutsung Liao (University of Chicago, Chicago, IL), and pMCSG7 from Dr. Frank Collart (Argonne National Laboratory, Argonne, IL). pCMV-βgal was obtained from Invitrogen.

The pFLAG-SRC1-His was constructed by cloning the steroid receptor coactivator-1 (SRC1) fragment (residues 568–780) from pCR3.1.SRC1 into pFLAG-CMV2 (Sigma) and subsequently subcloning into pET28b (Novagen). pFLAG-ERα and pFLAG-ERβ used in transient transfections were constructed by subcloning full-length hERα (from HEGO/pSG5) or hERβ (from pCMV5-hERβ) into pCMV-FLAG-2. p6×His-ERα LBD used in the competitive binding assays was constructed by subcloning ERα LBD (residues 304–554) into pET15b (Novagen). The ERα LBD (residues 298–554; Y537S) used for crystallization was expressed from pMCSG7 (25) as a fusion protein with a 23-residue N-terminal tag. The Y537S mutation was introduced to increase the solubility and yield of the ERα LBD for crystallization. From comparisons of the crystal structures of this mutant ER with wild type ER complexed to the same ligand, the mutation does not appear to cause significant changes to the overall conformation of the protein.[5]

Protein Expression and Purification for in Vitro Assays—Glutathione *S*-transferase (GST)-ERα LBD was expressed in *Escherichia coli* Rosetta cells (Novagen) by induction with 0.2 mM isopropyl-β-D-thiogalactopyranoside for 3 h at 25 °C. The protocol for the purification of the GST-ERα LBD was similar to that which has been described elsewhere (26). FLAG-SRC1, ERα LBD, and ERβ LBD were all expressed and purified as generally described. Proteins were expressed in Rosetta cells by induction with 0.6 mM isopropyl-β-D-thiogalactopyranoside for 3 h at 25 °C. Cell pellets were flash frozen in liquid nitrogen and stored at −80 °C. After thawing, they were resuspended in 5 volumes of lysis buffer (20 mM Tris buffer, pH 7.6, 500 mM NaCl, 10% (v/v) glycerol, 0.05% β-octyl glucoside, 10 mM imidazole, 10 mM β-mercaptoethanol (β-ME), 3 M urea (for ER LBD), protein inhibitor mixture (Calbiochem), 0.1 mg/ml lysozyme) and sonicated on ice three times for 30 s each. The lysates were centrifuged at 30,000 × *g* for 30 min to collect the supernatant, and the above procedure was repeated to extract additional soluble proteins from the cell debris. The two supernatant fractions were pooled and loaded on Ni^{2+}-nitrilotriacetic acid resin (Qiagen) pre-equilibrated with lysis buffer. The resin was washed with 5 column volumes of wash buffer (50 mM Tris buffer, pH 7.6, 500 mM NaCl, 0.05% β-octyl glucoside, 20 mM imidazole, 10 mM β-ME, protein inhibitor mixture) and eluted with 10 column volumes of elution buffer (50 mM Tris, pH 7.6, 300 mM NaCl, 0.05% β-octyl glucoside, 250 mM imidazole, 4 mM tris(2-carboxyethyl)phosphine hydrochloride, protein inhibitor mixture). Collected fractions were analyzed by SDS-PAGE before selecting the purest protein fractions to concentrate. Additionally, ERα LBD and ERβ LBD were dialyzed in binding buffer (50 mM Tris pH 8.0, 100 mM NaCl, 0.01% β-octyl glucoside, and 0.1% (v/v) glycerol) and FLAG-SRC1 in HTRF buffer (50 mM HEPES, pH 7.4, 50 mM KCl, 0.1% (v/v) Tween 20, and 1 mM EDTA).

Homogenous Time-resolved Fluorescence (HTRF) Assays—The anti-FLAG-XL665 and anti-GST-Eu(K) antibodies were from Cisbio International (Gif/Yvette Cedex, France) and the Wallac 1420 MicroPlate Reader from PerkinElmer Life Sciences. FLAG-SRC1 and GST-ERα LBD were diluted in HTRF buffer that included 1 mM dithiothreitol and 1 mg/ml bovine serum albumin and preincubated with anti-FLAG-XL665 and anti-GST-Eu(K), respectively, for 1 h at 4 °C. The two mixtures were then combined with test ligands (0.5%, v/v) and 2 M KF solution and incubated at 4 °C for 1–2 h with agitation. The plates were read on a Wallac 1420 MicroPlate Reader. The extent of the specific fluorescence resonance energy transfer was determined by taking a ratio of the emission intensities at 665 and 615 nm and scaled by 10^4. EC_{50} values in this and other assays were determined from the data using SigmaPlot (Systat Software).

Competitive Binding Assays—His-tagged ERα LBD/ERβ LBD was diluted with binding buffer to 8–10 nM and added to the wells of nickel-coated FlashPlates (PerkinElmer Life Sciences). The proteins were incubated for ~2 h at 25 °C to allow the ER to bind. Plates were then washed five times with phosphate-buffered saline, before the addition of 1–2 nM [^{3}H]E2 and test ligand diluted in binding buffer. The ligands were incubated for 4 h at 25 °C or overnight at 4 °C, and the plates were analyzed with a MicroBeta Scintillation Counter (PerkinElmer Life Sciences). IC_{50} and K_i values were determined from the data using SigmaPlot (Systat Software).

Transient Transfection and Transactivation Assays—In the transient transfection of COS-7 and SKBR3 cells, DNA was delivered to the cells using PolyFect (Qiagen). In the case of SKBR3, 150 ng of p3×ERE-Luc, 30 ng of pFLAG-ERα/pFLAG-ERβ, and 30 ng of normalization plasmid (pCMV-βgal) were used. For the COS-7 ER assays, 300 ng of p3×ERE-Luc, 40 ng of pFLAG-ERα/pFLAG-ERβ, and 40 ng of pCMV-βgal were used. In the COS-7 androgen receptor (AR) assays, 150 ng of p3×ARE-Luc, 30 ng of pAR, and 30 ng of pCMV-βgal were used. Ligands that had

[5] S. S. Rajan, K. W. Nettles, R. W. Hsieh, and Geoffrey L. Greene, unpublished results.

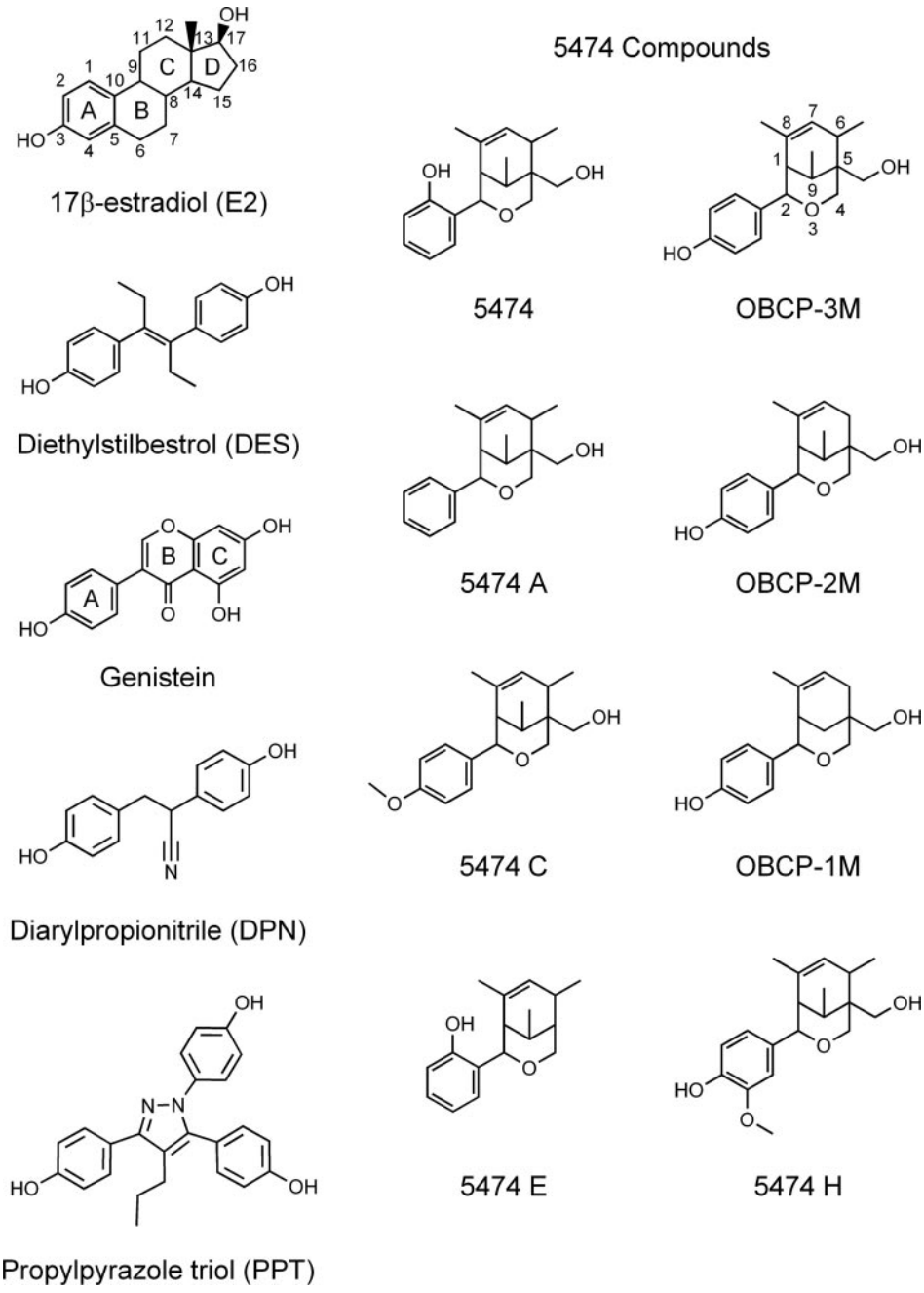

FIGURE 1. **Chemical structures of E2, DES, genistein, DPN, PPT, and the 5474 compounds.**

been diluted 1:200 in phenol red-free Dulbecco's modified Eagle's medium supplemented with 10% charcoal-stripped fetal bovine serum were added to the cells 18–24 h before cell harvest and lysis. Luciferase activities from lysed cells were analyzed on a MicroBeta (PerkinElmer Life Sciences) luminescence counter, and values were normalized with those from β-galactosidase activity (Promega).

Immature Rat Uterotrophic Growth Assays—Selected compounds were evaluated using the uterotrophic growth assay (27). Groups of immature Sprague-Dawley female rats (10 per group for vehicle, 5 per group all others) were injected subcutaneously with 10, 50, and 250 nmol of test ligand in 100 μl of vehicle (10% Cremaphor EL (Fluka Biochemicals), 88% phosphate-buffered saline, and 2% ethanol) daily for 3 consecutive days. Vehicle alone and E2 at doses of 1 and 10 nmol were administered in the same manner over the same period as controls. Animals were sacrificed on the fourth day, 24 h after the last injection. Uteri were removed, stripped free of fat and connective tissue, and blotted on filter paper, and wet weight was measured.

Quantitative Real Time Reverse Transcription-PCR Assays—U2OS-ERα and U2OS-ERβ cells (generous gifts from Drs. Thomas Spelsberg and David Monroe (Mayo Clinic, Rochester, MN)) were seeded in 6-well plates at $4-6 \times 10^4$ cells/well and pretreated for 24 h with 100 ng/ml doxycycline (Sigma). Cells were subsequently treated for an additional 24 h with ligands or vehicle (Me_2SO) control in the presence of 100 ng/ml doxycycline to maintain ER expression. Each treatment group was performed in triplicate. Total RNA was prepared with TRIzol reagent (Invitrogen). 2 μg of RNA was treated with DNase I (Invitrogen) before being reverse transcribed using the Superscript III First-Strand Synthesis System (Invitrogen). A combination of oligo(dT) and random hexamers was used to prime the cDNA synthesis reaction. The resultant cDNA products were diluted to 40 μl, and 5 μl of cDNA was used

in real time PCRs utilizing the QuantiTect SYBR Green PCR kit (Qiagen). The primer sequences used for real time PCR for angiotensinogen and β-actin have been previously reported by others (28). The reactions were carried out using the ABI 7300 Real-Time PCR System (Applied Biosystems) for 48 cycles (94 °C for 15 s, 54–58 °C for 30 s, 72 °C for 40 s) after an initial 15-min incubation at 95 °C. RNA levels were determined for angiotensinogen and β-actin RNA by comparison with standard curves generated from reference RNA (Stratagene). Angiotensinogen expression was then normalized to the endogenous reference gene β-actin, and the relative expression was then determined by normalizing to the Me_2SO-treated control.

Expression, Purification, and Crystallization of ERα LBD—hERα LBD was expressed in BL21(DE3) magic strain *E. coli* (29). Following isopropyl-β-D-thiogalactopyranoside induction, the cell pellets in 0.1 M HEPES, pH 7.5, 0.5 M NaCl, 10 mM β-ME, 5% (v/v) glycerol, and 10 mM imidazole were incubated with lysozyme (1 mg/ml) and protein inhibitor mixture (Sigma) and then sonicated. The ER protein was purified on a Ni^{2+}-nitrilotriacetic acid column (Qiagen), and the N-terminal polyhistidine tag was cleaved using tobacco etch virus protease (30), which carries a noncleavable polyhistidine tag. Following its separation from the protease and the tag on the Ni^{2+}-nitrilotriacetic acid column, the cleaved protein was diluted 1:10 in 25 mM Tris, pH 8.0, 0.1 M NaCl, 10 mM β-ME, and 5% (v/v) glycerol and purified further on a mono-Q anion exchange column (GE Healthcare) using an NaCl gradient of 25 mM to 0.6 M. The protein eluted at 0.3 M NaCl and was dialyzed in 4 mM HEPES, pH 7.5, 0.125 M NaCl, 10 mM β-ME, and 1.25% (v/v) glycerol. The protein was concentrated to ~10 mg/ml, incubated overnight with a 1 mM concentration of both the ligand and the GRIP1 peptide (residues 686–698) prior to screening for crystallization conditions in sitting drops (2:1 protein/reservoir) with the commercially available screens Index (Hampton Research) and Wizard (Emerald Biosystems) at both 16 and 25 °C. Optimization of initial screen conditions yielded diffraction quality crystals of ER in ~1 week at 16 °C in 0.2 M sodium malonate, 20% (w/v) polyethylene glycol 3350, pH 7.0, for OBCP-3M and in 0.2 M ammonium sulfate, 0.1 M Tris-HCl, 25% (w/v) polyethylene glycol 3350, pH 8.5, for OBCP-2M and OBCP-1M. Crystals were soaked in the mother liquor and 10% (v/v) glycerol prior to freezing in liquid nitrogen.

Data Collection, Structure Determination, and Refinement—Single wavelength (0.979 Å) native data sets were collected on a MarCCD detector at the 19-BM beamline (OBCP-3M) and on a Quantum 135 detector at the 14-BM beamline (OBCP-2M and OBCP-1M) of the Advanced Photon Source (Argonne National Laboratory). Data were collected with an oscillation of 1.5, 1.0, and 0.5° and an exposure of 10, 12, and 3 s per image, to a resolution of 2.25, 2.10, and 1.80 Å with average redundancies of 3.6, 5.1, and 3.6 for OBCP-3M, OBCP-2M, and OBCP-1M structures, respectively. Data were integrated and merged using HKL2000 (31) and then used in molecular replacement using MOLREP (32) with the ER structure from Protein Data Bank entry 1L2I as the search model for the OBCP-3M structure and 1ZKY as the search model for both the OBCP-2M and OBCP-1M structures. XtalView (33), CNS (version 1.1) (34), and REFMAC (35) programs were used for model building and refinement. Missing residues and alternate conformations for some side chains were manually modeled and refined in subsequent cycles. The missing residues in the final models are at the termini and surface loops. Details of diffraction data collection and processing of the ER crystal complexes are shown in Table 5. The ribbon diagram was prepared with Swiss-PdbViewer (36) and rendered in POV-RAY (Persistence of Vision Ray Tracer; available on the World Wide Web at www.povray.org). Figures showing electron density maps were prepared with BOBSCRIPT (37) and rendered in Raster3D (38). Structural alignments were performed with Swiss-PdbViewer and presented using MOLSCRIPT (39) and Raster3D.

TABLE 1
The ability of E2 and the 5474 compounds to promote interactions between SRC1 NRD and ERα LBD as measured in an HTRF assay

Compound	EC_{50}[a]
	nM
E2	0.37
OBCP-3M	7.0
OBCP-2M	9.3
OBCP-1M	13
5474	2000
5474A	800
5474C	4100
5474E	3200
5474H	290

[a] Data from the HTRF assays were expressed as ratios of emission intensity at 665 and 615 nm scaled by 10^4. Plots of these ratios *versus* ligand concentration were used to obtain EC_{50} values.

RESULTS

HTRF Screening with ERα LBD and SRC1 NRD to Identify ER Agonists—SRC1 nuclear receptor interaction domain (SRC1 NRD) is a protein fragment encompassing all three nuclear receptor box motifs (40) known to interact with the LBDs of nuclear receptors (41). To find ER agonists, compounds that promote the interaction between the ERα LBD and SRC1 NRD were identified using HTRF (42), a technology based on fluorescence resonance energy transfer. Of the 10,000 compounds screened in mixtures of eight compounds each (to give working concentrations of ~20 μM/compound), 40 mixtures increased HTRF signals to greater than 40% of the signal obtained with 10 nM E2 alone. We repeated the assay with each of the 320 compounds present in the original mixtures to select the 10 most active compounds. These compounds were tested over a range of concentrations to confirm dose-dependent promotion of ERα LBD/SRC1 NRD interactions. Compound 5474 (Fig. 1) was identified as the lead compound for structure activity relationship (SAR) studies.

SAR Studies on the 5474 Compound Family—Based on the core scaffold of 5474, we purchased or synthesized a variety of chemical analogs (Fig. 1) to evaluate the contributions of different functional groups to their activity, as assessed by the HTRF assay. Concentrations ranging from 0.1 nM to 100 μM were used to obtain EC_{50} values for each compound (Table 1). EC_{50} values reflect the potency of each compound in promoting the ERα LBD interaction with SRC1 NRD. A comparison of compounds 5474 and 5474E showed that removal of the hydroxymethyl group attached to the oxabicyclic scaffold resulted in a loss of activity. However, a greater impact occurred when the phenolic OH group was moved from the *ortho* position (5474) to the *para* position (OBCP-3M), which led to a nearly 300-fold increase in potency. Modifications of the phenolic ring of OBCP-3M, including removal of the OH group (5474A), methylation of the OH group (5474C), or the addition of a methoxy group to the ring (5474H), all resulted in a loss of activity. In contrast, the addition or subtraction of methyl groups from the oxabicyclic scaffold had a smaller impact on the EC_{50} values. Successive removal of methyl groups from the oxabicyclic scaffold of OBCP-3M resulted in progressively less activity.

OBCP Compounds Show ERβ Selectivity—The three most potent ligands from the SAR studies, OBCP-3M, OBCP-2M, and OBCP-1M (OBCP compounds) were evaluated in a competitive binding assay using [^{3}H]E2 to determine their affinities for the hERα and hERβ LBDs. Each compound was able to displace [^{3}H]E2 from recombinant ERα and ERβ LBD, suggesting that these compounds bind in the ligand-binding

pocket of the receptors. The K_i values of the compounds for ERα ranged from 560 to 1800 nM, and those for ERβ ranged from 12 to 190 nM (Table 2). All three compounds showed selectivity for ERβ, with preferences that ranged from ~10- to 50-fold (Table 2). These affinities and selectivities for ERβ are on the same order of magnitude as those for genistein, which binds ERα and ERβ with affinities of 530 and 7 nM, respectively, and is 76-fold ERβ-selective (Table 2).

OBCP Compounds Activate Full-length ERα and ERβ in Mammalian Cell Lines and Retain ERβ Selectivity—The OBCP compounds were also tested in transient transfection assays for their ability to activate ER transcription from a luciferase reporter under the control of a promoter containing three estrogen response elements (3×ERE). In COS-7 (monkey kidney) cells, all three compounds tested were agonists on full-length ERα and ERβ (Fig. 2, *A* and *B*). The selectivity of the OBCP compounds for ERβ activation, determined from their transcriptional potencies on each receptor, ranged from ~30- to 60-fold (Table 3). Efficacy on ERα transcription was comparable with E2, whereas for ERβ, transcription efficacy was 60–70% of the levels achieved by E2. To test for tissue-dependent effects, transient transfections using the same plasmids were carried out in SKBR3 (human breast cancer) cells with OBCP-3M and genistein. In this context, the ERβ selectivity of OBCP-3M (16-fold) was less than in the COS-7 model (29-fold) described above, and the efficacy profile of OBCP-3M also changed. In SKBR3 cells, OBCP-3M activated ERα and ERβ to 70% of the levels achieved by E2 (Fig. 2, *C* and *D*). Finally, in comparison with genistein, the ERβ selectivity of OBCP-3M was also lower (16- *versus* 48-fold) (Table 4).

OBCP Compounds Do Not Activate Androgen Receptor—To test whether OBCP compounds act specifically on ER, their ability to stimulate AR transcription was evaluated. AR, like ER, is a member of the NR3 nuclear receptor family. E2 binds with low affinity to AR but can activate AR transcription at high concentrations. However, none of the OBCP compounds activated AR at concentrations up to 50 μM (data not shown).

TABLE 2
ER binding and ERβ subtype selectivity of genistein and of OBCP compounds

Ligand	Receptor binding		
	ERα LBD K_i[a]	ERβ LBD K_i[a]	β selectivity[b]
	nM	*nM*	*-fold*
OBCP-3M	560	12	47
OBCP-2M	570	20	29
OBCP-1M	1800	190	9.5
Genistein	530	7.0	76

[a] K_i values were calculated using IC_{50} values determined in competitive binding assays between test ligands and [^{3}H]E2 on ERα or ERβ. The binding affinity (K_d) of [^{3}H]E2 to receptor was 3 nM (ERα) and 4 nM (ERβ).
[b] β selectivity is determined from the ratio K_i(ERα)/K_i(ERβ).

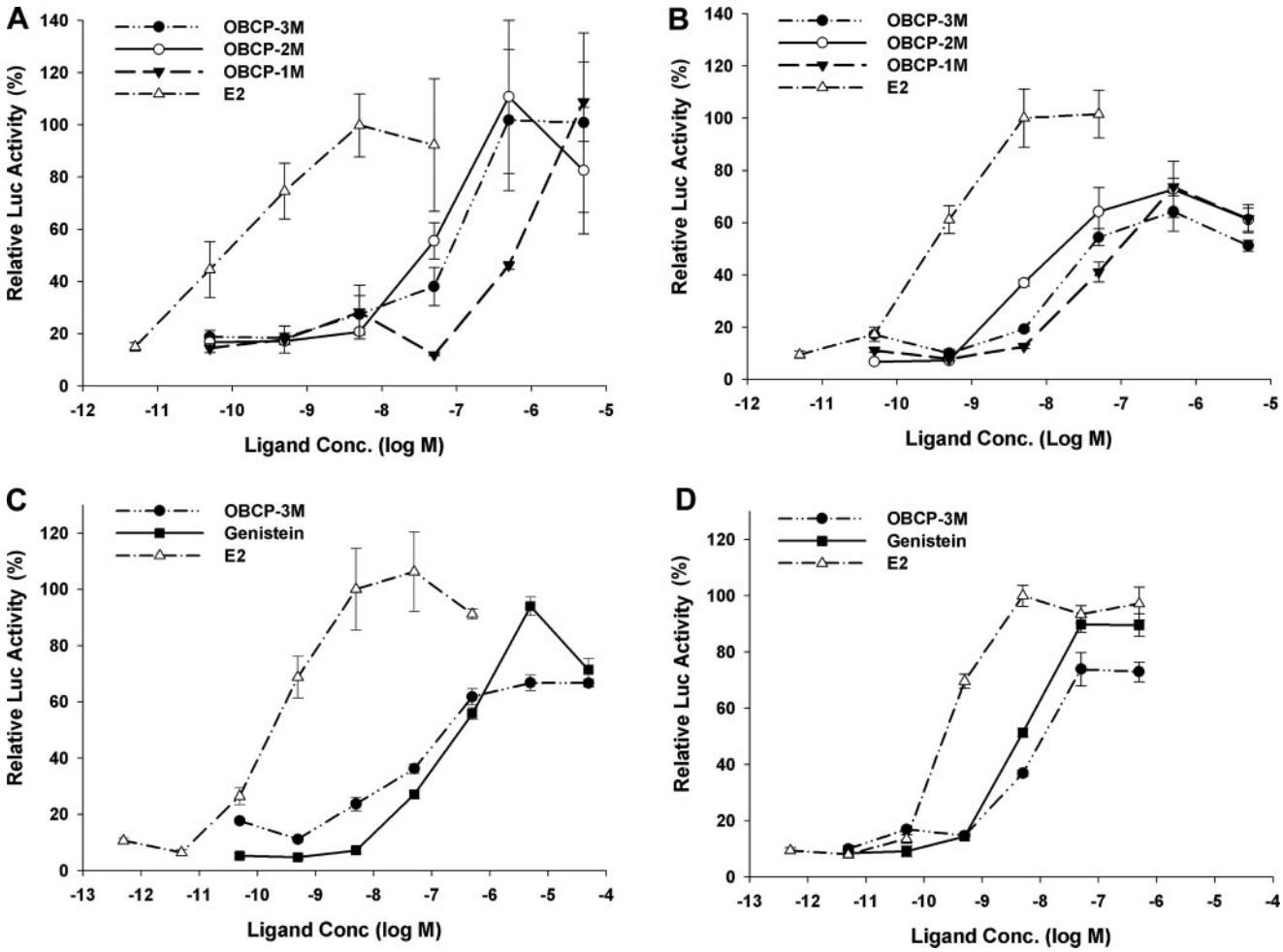

FIGURE 2. **Transcriptional activity of ERα and ERβ.** Mammalian cells were transfected with expression vectors for full-length ER, 3×ERE-Luc reporter, and control β-galactosidase expression plasmid. Shown are ERα (*A*) and ERβ (*B*) transcriptional activity with OBCP compounds and E2 in COS-7 cells. Also shown are ERα (*C*) and ERβ (*D*) transcriptional activity with OBCP-3M, genistein, and E2 in SKBR3 cells. Luciferase activities were normalized against β-galactosidase activity to correct for transfection efficiency. Relative luciferase activity values shown are the mean ± S.E. expressed as a percentage of the ERα or ERβ response with 5 nM E2.

TABLE 3

Transcriptional potency and selectivity of OBCP compounds and of E2 on full-length (FL) ER in COS-7 cells

Ligand[a]	FL hERα REP[b]	FL hERβ REP[b]	β selectivity[c]
	%	%	-fold
E2	100	100	1
OBCP-3M	0.11	3.1	29
OBCP-2M	0.16	8.5	55
OBCP-1M	0.014	0.84	59

[a] Transcriptional activities of ligands were measured using luciferase reporter plasmids containing the consensus 3×ERE promoter.
[b] Relative estrogenic potency (REP) = (EC_{50}(E2)/EC_{50}(ligand)) × 100. EC_{50} values were from the data shown in Fig. 2, *A* and *B*.
[c] β selectivity is determined from the ratio REP(ERβ)/REP(ERα).

TABLE 4

Transcriptional potency and selectivity of E2, OBCP-3M, and genistein on full-length ER in SKBR3 cells

Ligand[a]	FL-hERα REP[b]	FL-hERβ REP[b]	β selectivity[c]
	%	%	-fold
E2	100	100	1
OBCP-3M	0.35	5.6	16
Genistein	0.14	6.6	48

[a] Transcriptional activities of ligands were measured using luciferase reporter plasmids containing the consensus 3×ERE promoter.
[b] Relative estrogenic potency (REP) = (EC_{50}(E2)/EC_{50}(ligand)) × 100. EC_{50} values were from the data shown in Fig. 2, *C* and *D*.
[c] β selectivity is determined from the ratio REP(ERβ)/REP(ERα).

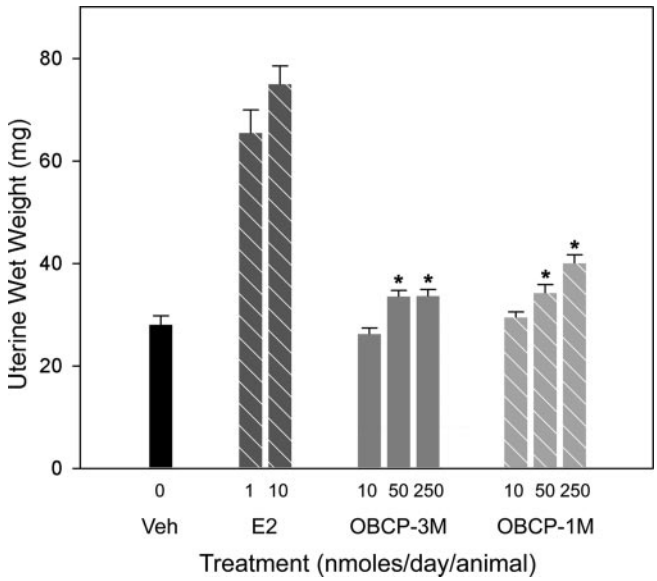

FIGURE 3. **Uterotrophic activity of OBCP-3M and OBCP-1M.** Immature rats were treated subcutaneously with the indicated doses for 3 days, and uterine wet weights were determined 24 h after the last dose was administered. Values represent the mean ± S.D. with 10 animals/group for the vehicle control and 5 animals/group for all others. *, value significantly different from vehicle control group ($p < 0.05$).

OBCP-3M and OBCP-1M Have Very Weak Uterotrophic Activity in Immature Sprague-Dawley Rats—To test OBCP compounds *in vivo*, we used a rat uterotrophic assay (27), which measures estrogenic activity based on the increase in uterine weight in immature rats (43). In contrast to E2, which at a dose of 1 nmol/animal/day increased uterine weight nearly 3-fold relative to vehicle control, both OBCP-3M and OBCP-1M were very weakly uterotrophic (~1.2- to 1.5-fold weight increase). These compounds stimulated significant uterine growth only at doses of 50 nmol/animal/day or greater (Fig. 3).

OBCP-3M Stimulates Expression of a Previously Identified Endogenous ERβ Target Gene—To test the effect of OBCP compounds on an endogenous ERβ gene target, we utilized two stably transfected U2OS cell lines containing doxycycline-inducible ERα (U2OS-ERα) or ERβ (U2OS-ERβ). These cell lines (28) and other similar U2OS cell lines (44, 45) have been previously used to identify genes regulated by specific ER subtypes. In these studies, angiotensinogen was shown to be a gene specifically up-regulated by E2 stimulation in the U2OS-ERβ cells but not the U2OS-ERα cells (28). We monitored its expression to determine whether OBCP-3M had an effect on this ERβ gene target. As controls, a non-subtype-selective agonist (E2), an ERα-selective agonist (PPT) (46), and an ERβ-selective agonist (DPN) (47) were also tested on both cell lines. The expression of angiotensinogen in U2OS-ERα cells was unaffected by any of the treatments relative to the effects of the vehicle treatment (Fig. 4*A*), consistent with its identification as an ERβ gene target. However, treatment of cells with E2, DPN, and OBCP-3M stimulated gene expression of angiotensinogen in the U2OS-ERβ cells to a higher level than that found in vehicle treated cells (Fig. 4*B*). Unexpectedly, treatment with PPT caused a decrease in the expression of angiotensinogen in the U2OS-ERβ cells relative to vehicle-treated cells.

Structure Determination of ERα LBD Complexes with GRIP1 Peptide and the OBCP-3M, OBCP-2M, and OBCP-1M Ligands—The crystal structures of the OBCP-3M-ERα LBD-GRIP1, OBCP-2M-ERα LBD-GRIP1, and OBCP-1M-ERα LBD-GRIP1 complexes were determined to identify conformational changes that could explain differences between the ERβ binding selectivity of OBCP-3M (47-fold), OBCP-2M (29-fold), and OBCP-1M (9.5-fold). Details of x-ray diffraction data collection, processing, and refinement of all three complexes are presented in Table 5. These high resolution ERα LBD structures have overall conformations similar to those found in structures of ERα complexed with the agonists E2 and diethylstilbestrol (DES) (13, 48). Thus, helix 12 packs against helices 3, 5, 6, and 11 to form a hydrophobic groove that accommodates the binding of the α-helical GRIP1 coactivator peptide (Fig. 5). The OBCP-3M, OBCP-2M, and OBCP-1M complexes are very similar to one another and can be superimposed via their backbone atoms with root mean square deviations of <0.50 Å.

Ligand-binding Regions of OBCP-3M, OBCP-2M, and OBCP-1M Structures—The $F_o - F_c$ electron density omit maps show the quality of the models and fit of the ligands in the electron density (Fig. 6). Important ligand-protein interactions seen in E2-ERα structures (Protein Data Bank code 1ERE) are preserved in the OBCP-3M, OBCP-2M, and OBCP-1M structures. For example, the phenolic OH group in all three OBCP ligands participates in a hydrogen bond network that includes Glu-353, Arg-394, and an ordered water molecule. On the opposite side of the pocket, the OBCP hydroxymethyl group forms a hydrogen bond with His-524 (Fig. 6). The bulk of the oxabicyclic scaffolds of the OBCP ligands lies almost entirely above and below the areas that would be occupied by the C- and D-rings of E2 (Fig. 7*B*). The oxabicyclic scaffold is involved in extensive hydrophobic interactions with residues that line the ligand-binding pocket.

Different Diastereomers of OBCP-3M and OBCP-2M Bind to Each Monomer in the ERα LBD Dimer—The OBCP-3M, OBCP-2M, and OBCP-1M compounds used in our studies are all mixtures of diastereomers. Interestingly, in the OBCP-3M and OBCP-2M complexes, two different diastereomers of the respective ligands are bound to each monomer of the ERα LBD dimer. In the OBCP-3M structure, the two diastereomers differ at the C-2 chiral center of the oxabicyclic scaffold, where the phenol ring is attached. Monomer A (MonA) of the ERα LBD dimer contains the C-2*R* diastereomer, and monomer B (MonB) contains the C-2*S* diastereomer. When MonA and MonB are superimposed, the two diastereomers can be seen to retain the same hydrogen

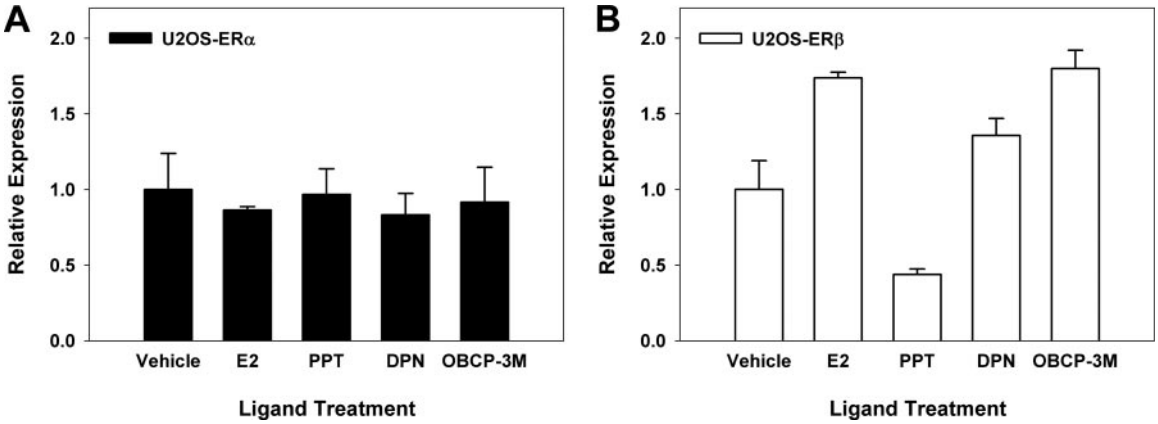

FIGURE 4. **Relative expression levels of a previously identified endogenous ERβ target gene in U2OS cells in response to ligands.** U2OS cells with doxycycline-inducible ERα (U2OS-ERα) or ERβ (U2OS-ERβ) were pretreated with 100 ng/ml doxycycline for 24 h followed by treatment with vehicle control (Me_2SO), E2 (10 nM), PPT (10 nM), DPN (10 nM), or OBCP-3M (50 nM) in the presence of doxycycline for an additional 24 h. Cells were harvested, and real time reverse transcription-PCR was performed using primers specific for the ERβ target gene angiotensinogen and the housekeeping gene β-actin. For both U2OS-ERα (*A*) and U2OS-ERβ (*B*), angiotensinogen expression was normalized to β-actin expression, and the relative expression was determined by normalizing to the vehicle control. Each treatment group was performed in triplicate, and values represent the mean ± S.E.

TABLE 5

Summary of the crystallographic data: Diffraction data collection parameters, processing, and refinement statistics for the ligand-ERα LBD-GRIP1 crystal complexes

	OBCP-3M-ERα-GRIP1	OBCP-2M-ERα-GRIP1	OBCP-1M-ERα-GRIP1
Data collection			
Space group	$P2_1$	$P2_1$	$P2_1$
Unit cell			
a, *b*, *c* (Å)	55.93 84.13 58.22	56.40 81.81 58.86	55.96 83.96 58.24
β (degrees)	109.06	111.16	108.81
Protein molecules/asymmetric units	2	2	2
Wavelength (Å)	0.979	0.979	0.979
Data processing			
Resolution range (Å)	30.0-2.25 (2.31-2.25)[a]	30.0-2.10 (2.18-2.10)[a]	30.0-1.80 (1.86-1.80)[a]
Reflections	24,141	29,195	46,440
Completeness (%)	95.9 (59.7)[a]	98.9 (100.0)[a]	98.81 (94.02)[a]
R_{merge} (%)[b]	11.8 (56.4)[a]	10.2 (42.1)[a]	7.3 (40.7)[a]
Refinement			
Resolution range (Å)	27.0-2.25	19.6-2.10	20.0-1.80
Reflections	22,883	27,374	44,059
R_{work} (%)	18.5 (26.5)[a]	20.0 (21.9)[a]	20.3 (23.6)[a]
R_{free} (%)	23.1 (36.2)[a]	24.0 (29.6)[a]	23.8 (30.0)[a]
Root mean square deviation			
Bond lengths (Å)	0.011	0.008	0.005
Bond angles (degrees)	1.171	1.074	0.927
Mean *B* factor	28.76	42.09	27.48
Waters	144	25	91
Protein Data Bank code	1ZKY	2FAI	2B1V

[a] Highest resolution shell.
[b] $R_{merge} = \Sigma|I(k) - [I]|/\Sigma I(k)$, where $I(k)$ is the value of the kth measurement of the intensity of a reflection, $[I]$ is the mean value of the intensity of that reflection, and Σ is of all of the measurements. $R_{factor} = \Sigma|F_o - F_c|/\Sigma|F_o|$.

bond contacts, despite different orientations of the OBCP-3M oxabicyclic scaffolds (Fig. 7*A*). This can occur because the phenolic OH and the hydroxymethyl OH of the two diastereomers are similarly positioned within each monomer. The major difference between the two monomers is that in MonA, the 6-methyl of OBCP-3M displaces the side chain of Met-343, which subsequently displaces that of Met-342. However, this change only locally perturbs the ERα LBD structure and does not affect the overall structure of the dimer. In contrast to findings in the OBCP-3M structure, the OBCP-2M oxabicyclic scaffold is bound to each monomer in a similar orientation. However, the electron density of the ligand in MonB appears to be produced by a combination of two OBCP-2M diastereomers that differ in the attachment of a methyl group at the C-9 chiral center. Thus, whereas MonA contains the C-9*R* diastereomer, Mon B is occupied by a mixture of the C-9*S* (Fig. 6*C*) and C-9*R* diastereomers. Interestingly, in the OBCP-1M complex, the same stereoisomer is bound to each monomer.

DISCUSSION

We have identified and characterized the biological activities and mechanisms of action of a family of ERβ-selective agonists that have a nonplanar oxabicyclic scaffold. These compounds bind in the ligand-binding pocket of ER and induce an agonist conformation of the receptor (Fig. 5) that permits the recruitment of coactivators such as SRC1 or GRIP1 via their nuclear receptor box motifs. The most selective and potent of these compounds, OBCP-3M, exhibited a ~50-fold selectivity for ERβ in binding assays.

Cell-based experiments using full-length ERs show that OBCP-3M and its analogs retain their ERβ-selective activity and are able to activate ER transcription through a promoter containing the consensus 3×ERE motif. This activity is specific to ER, since no activity is seen with AR. In addition, OBCP-3M exhibits some degree of tissue-dependent activity. In COS-7 cells, OBCP-3M acts as a full agonist on ERα and as a partial agonist on ERβ (Fig. 2, *A* and *B*) with a ~ 30-fold ERβ selectivity (Table

3). However, in SKBR3 cells, OBCP-3M is a partial agonist on both ERα and ERβ (Fig. 2, *C* and *D*) and shows only 16-fold ERβ selectivity (Table 4). The differences in the selectivity and efficacy of OBCP-3M in these two cell contexts may be due to the different tissue and species origins of the cell lines. Thus, differing compositions of coactivators in each cell line (49) and possible differences in coactivator recruitment by ER (50) are likely factors affecting the observed activity of OBCP-3M. Future studies to identify coactivators that preferentially interact with ER when OBCP-3M or its analogs are bound may help optimize these compounds for cell- or tissue-selective activity.

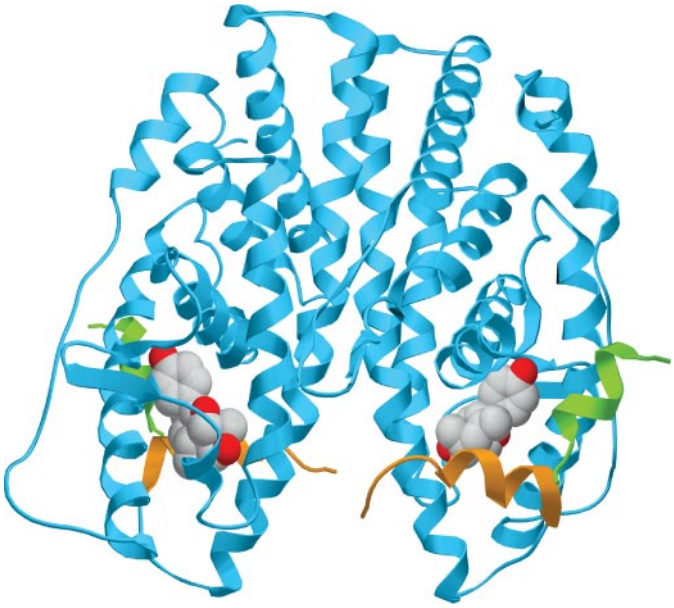

FIGURE 5. **ERα ligand binding domain dimer.** Shown are *ribbon diagrams* of the ERα-LBD dimer (*turquoise*) and peptide fragments of the GRIP1 coactivator protein (*green*) in complex with OBCP-3M (*space-filled model*). The position of helix 12 (*gold*) of the LBD shows that it is in the agonist conformation. Monomer A is shown on the *left*, and monomer B is shown on the *right*.

The observation that OBCP-3M and OBCP-1M are only weakly stimulatory in uterine growth assays (Fig. 3) is consistent with findings from previous studies of subtype-selective compounds. Those studies demonstrated that uterine growth stimulation is mainly associated with ERα activity (10). The low level of uterotrophic activity exhibited at higher ligand doses is probably due to their residual ERα activity, an effect also seen with other ERβ-selective ligands (11). However, our results do not preclude the possibility that the weaker activity compared with E2 can be due to differences in the absorption, distribution, metabolism, or excretion of the compounds.

Experiments in U2OS-ERα and U2OS-ERβ cells provide further support for our *in vivo* findings and suggest that OBCP-3M can stimulate ERβ activity. Treatment of U2OS-ERβ cells with OBCP-3M showed that the compound can activate ERβ to up-regulate the expression of angiotensinogen, a previously identified ERβ target gene (28). Additional studies on the expression of other endogenous ERβ target genes would better define the ERβ-selective properties of the OBCP compounds.

SAR studies examining the different analogs within the 5474 compound family indicate that two functional groups on the OBCP ligands are important for binding to the ERα LBD: the phenol ring and the hydroxymethyl group at the C-2 and C-5 positions, respectively, of the oxabicyclic scaffold. Whereas the former is critical for strong interactions of the OBCP compounds with the ERα LBD, the hydroxymethyl

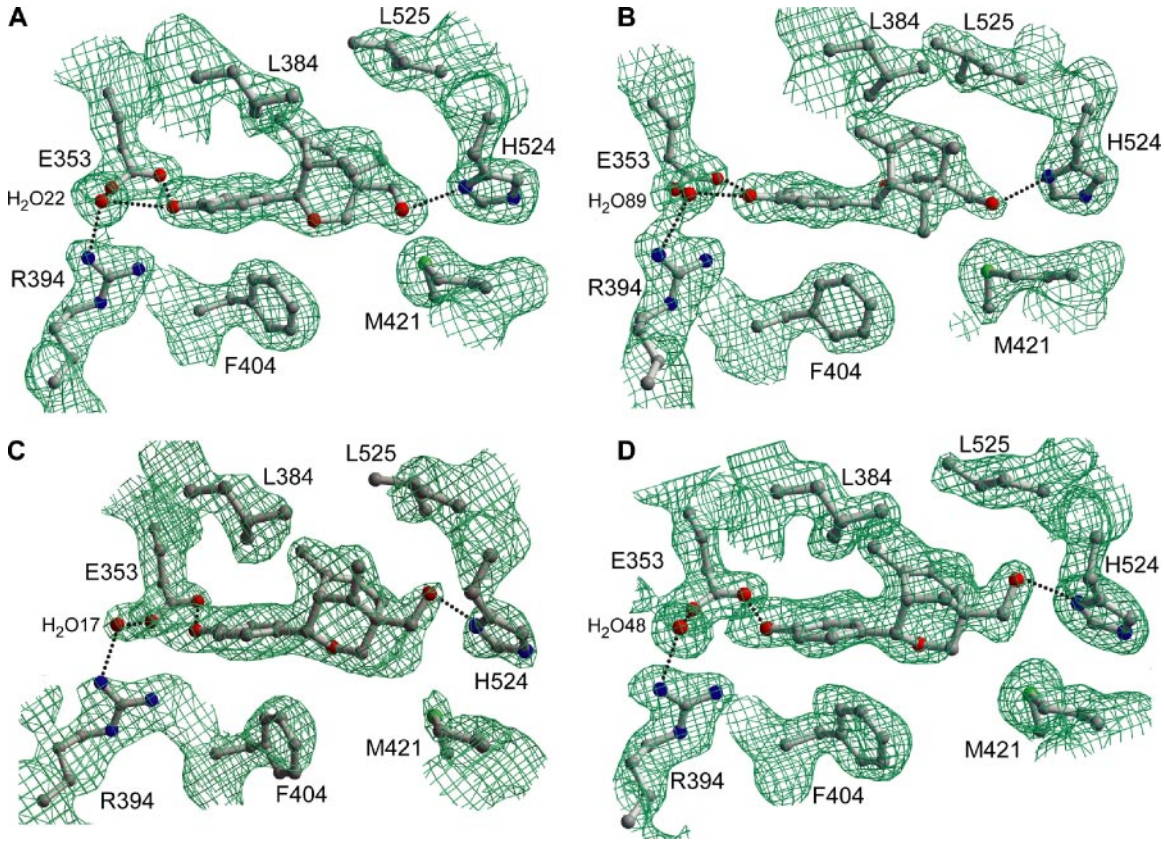

FIGURE 6. **ERα ligand binding site.** Shown are *ball-and-stick renderings* of the ligands OBCP-3M(MonA) (*A*), OBCP-3M(MonB) (*B*), OBCP-2M(MonB) (*C*) (only the C9-*S* diastereomer shown), and OBCP-1M (*D*), along with their interacting residues and corresponding $F_o - F_c$ electron density omit maps contoured at 1.95σ (OBCP-3M), 1.35σ (OBCP-2M), and 1.80σ (OBCP-1M). Hydrogen bonds are shown as *dotted lines*.

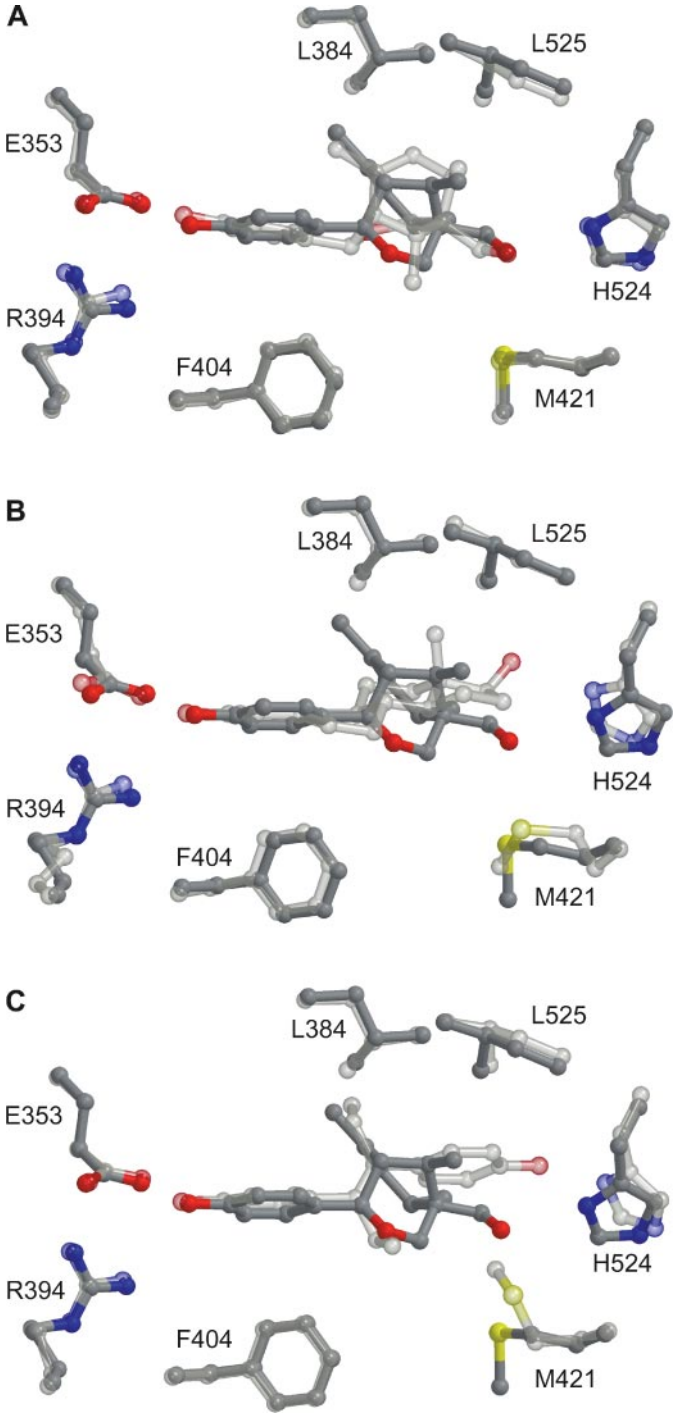

FIGURE 7. **Ligand binding mode of OBCP-3M.** Monomer A of OBCP-3M-ERα LBD-GRIP1 complex (*dark gray*) was superimposed on monomer B of the same complex (*A*) and with other ERα structures complexed with E2 (Protein Data Bank code 1ERE) (*B*) and DES (Protein Data Bank code 3ERD) (*C*) (all *light gray*). Shown are the *ball-and-stick diagrams* of their ligand binding sites.

group enhances the binding of these ligands. Based on the mechanisms by which E2 binds the ERα LBD (13), we predicted that the *para* phenolic OH group of the OBCP ligands probably mimics the binding mode of the E2 A-ring 3-OH, whereas the OH of the hydroxymethyl group binds in a similar mode as the 17β-OH of E2. Crystal complexes of ERα LBD-GRIP1 with OBCP-3M, OBCP-2M, and OBCP-1M confirmed these predictions (Figs. 5 and 6*B*). These structures also show that the oxabicyclic scaffolds of the OBCP ligands occupy some of the vacant space that would surround the C- and D-ring positions of E2 (13) in the ligand binding pocket (Fig. 7*B*).

An unexpected and interesting finding was that in both the OBCP-3M and OBCP-2M structures, different diastereomers of the ligands bind each monomer of the ERα LBD dimer. Another nuclear receptor, the pregnane X receptor, was shown previously to bind the compound SR12813 in a number of different orientations (51), but to our knowledge, this is the first report of a nuclear receptor binding two different stereoisomers in a dimer. Surprisingly, the OBCP-1M complex, which also crystallized in the presence of a mix of diastereomers and packed in the same space group with similar cell dimensions as the OBCP-3M and OBCP-2M complexes, bound the same stereoisomer in each monomer. In the OBCP-2M structure, the two diastereomers found in MonB bind in the same general orientation and differ only in the position of the methyl attached to the C-9 chiral center. In contrast, in the OBCP-3M structure, each diastereomer binds its monomer in a very different orientation (Fig. 6, *A* and *B*). In this case, the unique binding of OBCP-3M is probably due to the symmetry conferred on its six-membered ring (C1-C9-C5-C6-C7-C8) by the three methyl groups. This symmetry, which is lacking in OBCP-2M and OBCP-1M, allows the substitution of methyl groups in making ligand-protein contacts when different diastereomers bind the receptor. Comparative structural analysis of the two monomers (Fig. 7*A*) shows that the receptor contacts made by the 8-methyl and 9-methyl groups of OBCP-3M(MonA) are equivalent to those made by the 8-methyl and 6-methyl groups, respectively, of OBCP-3M(MonB). The third methyl group in each diastereomer, the 6-methyl of OBCP-3M(MonA) and the 9-methyl of OBCP-3M(MonB), make unique contacts with the receptor that have no equivalent in the other diastereomer. However, these interactions cause only local changes to the ligand-binding structure and do not affect the overall conformation of the two monomers. Selection for one diastereomer of OBCP-3M over the others in each monomer is an interesting crystallographic finding, because such microheterogeneity in the protein samples often interferes with crystallization or results in poor crystal order (52).

Comparative structural analyses of the three OBCP-ERα LBD structures with other ER structures suggest that the ERβ selectivity of the OBCP ligands can be attributed to the two residues that differ in the ligand-binding pockets of the ER subtypes. Of these, the difference at Leu-384(ERα)/Met-336(ERβ) probably contributes the most to the subtype selectivity of the OBCP ligands. Among the ERα structures, the Leu-384 side chain positions are essentially unchanged whether OBCP ligands or non-subtype-selective ligands, such as E2 or DES, are bound (Fig. 5, *B* and *C*). Leu-384 does not interact with E2 and interacts weakly with DES. Similarly, the OBCP ligands interact with Leu-384 through weak van der Waal contacts made by the 8-methyl groups of OBCP-3M(MonB), OBCP-2M, and OBCP-1M. However, superimposing ERβ (Protein Data Bank code 1X7J) onto the OBCP-ERα structures shows that the change to Met-336 in ERβ at the equivalent position to Leu-384 in ERα places the larger methionine close enough (~3–4 Å) to make van der Waal contacts with the OBCP ligands (Fig. 8). The flexibility observed for the Met-336 side chain (14) suggests that it can easily move to accommodate the oxabicyclic scaffold of the OBCP ligands. Thus, Met-336 could make extensive contacts with the hydrophobic surfaces of these ligands. These interactions would favor the binding of OBCP ligands to ERβ. The additional contacts made by the extra methyl groups of OBCP-3M and OBCP-2M probably account for their increased affinity and improved ERβ selectivity compared with OBCP-1M. In comparison, the bulk of the DES and E2 structures are too far away to make productive contacts with Met-336; E2 has only

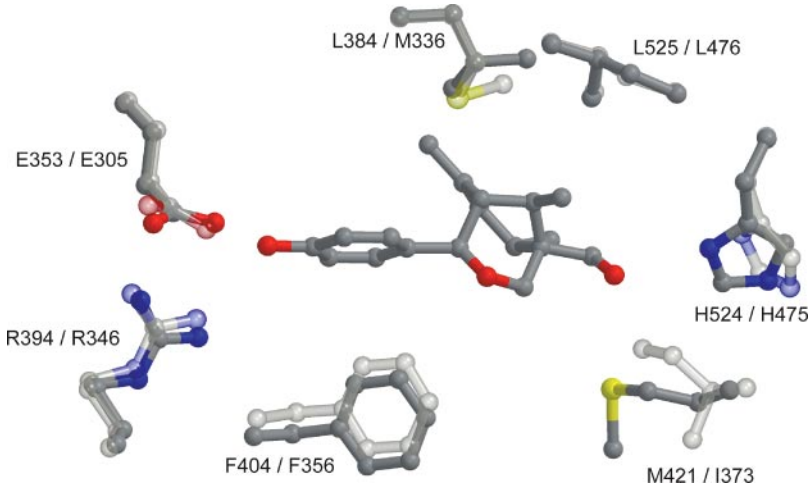

FIGURE 8. **Potential interactions of OBCP-3M(MonA) with residues in the ERβ ligand binding site.** The OBCP-3M-ERα LBD-GRIP (MonA) complex was superimposed on the genistein-ERβ LBD-SRC3 complex (Protein Data Bank code 1X7J) by aligning their protein backbone atoms (root mean square deviation of 1.04 Å over 916 atoms). Shown are *ball and stick diagrams* of the ligand binding site of ERα LBD with OBCP-3M(MonA) (*dark gray*) superimposed on the ligand binding site of ERβ LBD (*light gray*). The structure of genistein has been omitted from the ERβ structure for clarity.

a 13β-methyl group and DES an ethyl group with which Met-336 could interact.

Met-421 (Ile-373 in ERβ) also affects the ERβ selectivity of the OBCP ligands. Superimposed structures of DES- or E2-ERα LBD with the OBCP structures show that the OBCP ligands would sterically clash with Met-421 if the residue is positioned as seen in structures with non-subtype-selective ligands (DES/E2) (Fig. 7, *B* and *C*). These steric clashes are with the ring atoms on the oxabicyclic scaffold (~2.5–3.5 Å) and the methyl of the hydroxymethyl group (<2 Å) of these compounds. To minimize such steric collisions with the OBCP ligands, the Met-421 side chains in the OBCP complexes are rotated away from the positions that they adopt in the DES/E2 structures (Fig. 7). However, in the OBCP-3M structure, the OH of the hydroxymethyl group is also positioned in close proximity to Met-421 (3.8 Å). This close approach probably results in electrostatic repulsion between the partial negative charges carried by the oxygen of the OH group and the sulfur of the methionine group. The hydroxymethyl group of OBCP-3M is limited in its ability to reduce this repulsion by rotating away because of steric constraints imposed by the two surrounding 6- and 9-methyl groups. In contrast, with only one or no methyl groups nearby, the hydroxymethyl of OBCP-2M and OBCP-1M can freely rotate to position itself away from the sulfur of Met-421 (5.0 Å) and toward His-524. Here, the oxygen of the hydroxymethyl experiences weaker electrostatic repulsions with the methionine and can hydrogen-bond with His-524. The replacement of Met-421 in ERα by Ile-373 in ERβ would eliminate the repulsive forces experienced by the OBCP-3M OH because isoleucine is nonpolar and shorter and occupies less volume than methionine. This substitution relieves OBCP-3M of its electrostatic repulsion in ERα (but minimally affects OBCP-1M and OBCP-2M) and would contribute to the stronger selectivity of OBCP-3M for ERβ.

ERβ-selective agonists can use three major mechanisms to take advantage of the two residues that differ between the ligand-binding pockets of ERα and ERβ. The first mechanism is to promote unfavorable interactions with ERα. This is the primary mechanism used by the benzoxazole/benzofuran compounds (17) (Fig. S1), in which acetonitrile/vinyl groups are positioned near Met-421, and by 8β-vinyl estradiol (11) (Fig. S1), in which a vinyl group clashes with Leu-384. The second mechanism is to promote favorable interactions with ERβ. These are the proposed mechanisms used by DPN (53) (Fig. 1) and genistein (21), in which a polarizable nitrile group and an aromatic (B) ring, respectively, interact with Met-336. The third mechanism is to combine the aforementioned two mechanisms. We have observed this combination with OBCP-3M, and it has also been described as the secondary mechanism for the benzoxazole/benzofuran ligands (17). Our structural analyses suggest that the ERβ selectivity of the OBCP ligands results mainly from favorable interactions with Met-336 in ERβ, because this interaction is common to these ligands. However, the greater ERβ selectivity of OBCP-3M compared with its analogs is probably achieved by the additional unfavorable interaction made with Met-421 in ERα. Although the ERβ selectivity of OBCP-3M is modest, we believe that optimization of each of its interactions would improve its selectivity.

The identification of OBCP-3M and its analogs adds to the repertoire of bicyclic ligands that have been reported (54–57), including a very recent report on similar oxabicyclic compounds (22). Promising results from our biological studies and those of others (22) suggest that the oxabicyclic compounds have potential as lead compounds in the development of subtype-selective ligands for investigative or therapeutic purposes. Our crystallographic studies show for the first time how ligands with bulky bicyclic scaffolds can be accommodated in the flexible ligand-binding pocket of ER and suggest how these ligands interact with both Met-421(ERα) and Met-336(ERβ) to achieve ERβ selectivity. These findings should stimulate interest in ligands that can utilize regions of the ER ligand-binding pocket that remain unoccupied when planar ligands are bound (13). Our studies should facilitate the structure-based design of more potent and subtype-selective ER modulators belonging to this relatively new structural class.

Acknowledgments—We thank Drs. Andzrej Joachimiak and Frank Collart (Argonne National Laboratory) for the use of materials and facilities at Argonne National Laboratory, Drs. Ning Lei and Vukica Srajer (Argonne National Laboratory) for assistance at BioCARS, Drs. Ronghuang Zhang and Youngchang Kim (Argonne National Laboratory) for assistance at Structural Biology Center, Dr. Kendall Nettles (Scripps Research Institute) and Johnnie Hahm for plasmid design and construction, Dr. Jaime Zhou (University of Chicago) for help with the real time PCR equipment, Dr. Hoyee Leong and Priya Mathur (University of Chicago) for advice on real time PCR, Dr. Woon-Seok Yeo (University of Chicago) for assistance and advice in chemical synthesis, Dr. Young-Sam Lee (University of Chicago) for assistance with screening, and Drs. Stephen Kent and Wei-Jen Tang (University of Chicago) for helpful comments. We also thank all of our colleagues who provided plasmids and cells used in this study.

REFERENCES

1. Couse, J. F., and Korach, K. S. (1999) *Endocr. Rev.* **20,** 358–417
2. Pearce, S. T., and Jordan, V. C. (2004) *Crit. Rev. Oncol. Hematol.* **50,** 3–22
3. Nemenoff, R. A., and Winn, R. A. (2005) *Eur. J. Cancer* **41,** 2561–2568

4. Kuiper, G. G., Carlsson, B., Grandien, K., Enmark, E., Haggblad, J., Nilsson, S., and Gustafsson, J. A. (1997) *Endocrinology* **138,** 863–870
5. Enmark, E., Pelto-Huikko, M., Grandien, K., Lagercrantz, S., Lagercrantz, J., Fried, G., Nordenskjold, M., and Gustafsson, J. A. (1997) *J. Clin. Endocrinol. Metab.* **82,** 4258–4265
6. Tremblay, G. B., Tremblay, A., Copeland, N. G., Gilbert, D. J., Jenkins, N. A., Labrie, F., and Giguere, V. (1997) *Mol. Endocrinol.* **11,** 353–365
7. Korach, K. S., Emmen, J. M., Walker, V. R., Hewitt, S. C., Yates, M., Hall, J. M., Swope, D. L., Harrell, J. C., and Couse, J. F. (2003) *J. Steroid Biochem. Mol. Biol.* **86,** 387–391
8. Rossouw, J. E., Anderson, G. L., Prentice, R. L., LaCroix, A. Z., Kooperberg, C., Stefanick, M. L., Jackson, R. D., Beresford, S. A., Howard, B. V., Johnson, K. C., Kotchen, J. M., and Ockene, J. (2002) *J. Am. Med. Assoc.* **288,** 321–333
9. Harris, H. A., Albert, L. M., Leathurby, Y., Malamas, M. S., Mewshaw, R. E., Miller, C. P., Kharode, Y. P., Marzolf, J., Komm, B. S., Winneker, R. C., Frail, D. E., Henderson, R. A., Zhu, Y., and Keith, J. C., Jr. (2003) *Endocrinology* **144,** 4241–4249
10. Harris, H. A., Katzenellenbogen, J. A., and Katzenellenbogen, B. S. (2002) *Endocrinology* **143,** 4172–4177
11. Hillisch, A., Peters, O., Kosemund, D., Muller, G., Walter, A., Schneider, B., Reddersen, G., Elger, W., and Fritzemeier, K. H. (2004) *Mol. Endocrinol.* **18,** 1599–1609
12. Hegele-Hartung, C., Siebel, P., Peters, O., Kosemund, D., Muller, G., Hillisch, A., Walter, A., Kraetzschmar, J., and Fritzemeier, K. H. (2004) *Proc. Natl. Acad. Sci. U. S. A.* **101,** 5129–5134
13. Brzozowski, A. M., Pike, A. C., Dauter, Z., Hubbard, R. E., Bonn, T., Engstrom, O., Ohman, L., Greene, G. L., Gustafsson, J. A., and Carlquist, M. (1997) *Nature* **389,** 753–758
14. Pike, A. C., Brzozowski, A. M., Hubbard, R. E., Bonn, T., Thorsell, A. G., Engstrom, O., Ljunggren, J., Gustafsson, J. A., and Carlquist, M. (1999) *EMBO J.* **18,** 4608–4618
15. Veeneman, G. H. (2005) *Curr. Med. Chem.* **12,** 1077–1136
16. Mewshaw, R. E., Edsall, R. J., Jr., Yang, C., Manas, E. S., Xu, Z. B., Henderson, R. A., Keith, J. C., Jr., and Harris, H. A. (2005) *J. Med. Chem.* **48,** 3953–3979
17. Manas, E. S., Unwalla, R. J., Xu, Z. B., Malamas, M. S., Miller, C. P., Harris, H. A., Hsiao, C., Akopian, T., Hum, W. T., Malakian, K., Wolfrom, S., Bapat, A., Bhat, R. A., Stahl, M. L., Somers, W. S., and Alvarez, J. C. (2004) *J. Am. Chem. Soc.* **126,** 15106–15119
18. Henke, B. R., Consler, T. G., Go, N., Hale, R. L., Hohman, D. R., Jones, S. A., Lu, A. T., Moore, L. B., Moore, J. T., Orband-Miller, L. A., Robinett, R. G., Shearin, J., Spearing, P. K., Stewart, E. L., Turnbull, P. S., Weaver, S. L., Williams, S. P., Wisely, G. B., and Lambert, M. H. (2002) *J. Med. Chem.* **45,** 5492–5505
19. Malamas, M. S., Manas, E. S., McDevitt, R. E., Gunawan, I., Xu, Z. B., Collini, M. D., Miller, C. P., Dinh, T., Henderson, R. A., Keith, J. C., Jr., and Harris, H. A. (2004) *J. Med. Chem.* **47,** 5021–5040
20. Shiau, A. K., Barstad, D., Radek, J. T., Meyers, M. J., Nettles, K. W., Katzenellenbogen, B. S., Katzenellenbogen, J. A., Agard, D. A., and Greene, G. L. (2002) *Nat. Struct. Biol.* **9,** 359–364
21. Manas, E. S., Xu, Z. B., Unwalla, R. J., and Somers, W. S. (2004) *Structure* (*Camb.*) **12,** 2197–2207
22. Hamann, L. G., Meyer, J. H., Ruppar, D. A., Marschke, K. B., Lopez, F. J., Allegretto, E. A., and Karanewsky, D. S. (2005) *Bioorg. Med. Chem. Lett.* **15,** 1463–1466
23. Chauzov, V. A., and Parchinskii, V. Z. (1997) *Zhurnal Obshchei Khimii* **67,** 166–167
24. Chauzov, V. A., and Parchinskii, V. Z. (1996) *Zhurnal Obshchei Khimii* **66,** 2061–2062
25. Stols, L., Gu, M., Dieckman, L., Raffen, R., Collart, F. R., and Donnelly, M. I. (2002) *Protein Expression Purif.* **25,** 8–15
26. Lally, J. M., Newman, R. H., Knowles, P. P., Islam, S., Coffer, A. I., Parker, M., and Freemont, P. S. (1998) *Acta. Crystallogr. Sect. D Biol. Crystallogr.* **54,** 423–426
27. DeSombre, E. R., Mease, R. C., Sanghavi, J., Singh, T., Seevers, R. H., and Hughes, A. (1988) *J. Steroid Biochem.* **29,** 583–590
28. Monroe, D. G., Getz, B. J., Johnsen, S. A., Riggs, B. L., Khosla, S., and Spelsberg, T. C. (2003) *J. Cell. Biochem.* **90,** 315–326
29. Dieckman, L., Gu, M., Stols, L., Donnelly, M. I., and Collart, F. R. (2002) *Protein Expression Purif.* **25,** 1–7
30. Phan, J., Zdanov, A., Evdokimov, A. G., Tropea, J. E., Peters, H. K., 3rd, Kapust, R. B., Li, M., Wlodawer, A., and Waugh, D. S. (2002) *J. Biol. Chem.* **277,** 50564–50572
31. Otwinowski, Z., and Minor, W. (1997) *Methods Enzymol.* **276,** 307–326
32. Vagin, A., and Teplyakov, A. (1997) *J. Appl. Crystallogr.* **30,** 1022–1025
33. McRee, D. E. (1999) *J. Struct. Biol.* **125,** 156–165
34. Brunger, A. T. (1992) *Nature* **355,** 472–475
35. Murshudov, G. N., Vagin, A. A., and Dodson, E. J. (1997) *Acta Crystallogr. D Biol. Crystallogr.* **53,** 240–255
36. Guex, N., and Peitsch, M. C. (1997) *Electrophoresis* **18,** 2714–2723
37. Esnouf, R. M. (1997) *J. Mol. Graph. Model.* **15,** 132–134
38. Merritt, E. A., and Bacon, D. J. (1997) *Method. Enzymol.* **277,** 505–524
39. Kraulis, P. (1991) *J. Appl. Crystallogr.* **24,** 946–950
40. Heery, D. M., Kalkhoven, E., Hoare, S., and Parker, M. G. (1997) *Nature* **387,** 733–736
41. Onate, S. A., Boonyaratanakornkit, V., Spencer, T. E., Tsai, S. Y., Tsai, M. J., Edwards, D. P., and O'Malley, B. W. (1998) *J. Biol. Chem.* **273,** 12101–12108
42. Zhou, G., Cummings, R., Li, Y., Mitra, S., Wilkinson, H. A., Elbrecht, A., Hermes, J. D., Schaeffer, J. M., Smith, R. G., and Moller, D. E. (1998) *Mol. Endocrinol.* **12,** 1594–1604
43. Reel, J. R., Lamb, I. J., and Neal, B. H. (1996) *Fundam. Appl. Toxicol.* **34,** 288–305
44. Kian Tee, M., Rogatsky, I., Tzagarakis-Foster, C., Cvoro, A., An, J., Christy, R. J., Yamamoto, K. R., and Leitman, D. C. (2004) *Mol. Biol. Cell* **15,** 1262–1272
45. Stossi, F., Barnett, D. H., Frasor, J., Komm, B., Lyttle, C. R., and Katzenellenbogen, B. S. (2004) *Endocrinology* **145,** 3473–3486
46. Stauffer, S. R., Coletta, C. J., Tedesco, R., Nishiguchi, G., Carlson, K., Sun, J., Katzenellenbogen, B. S., and Katzenellenbogen, J. A. (2000) *J. Med. Chem.* **43,** 4934–4947
47. Meyers, M. J., Sun, J., Carlson, K. E., Marriner, G. A., Katzenellenbogen, B. S., and Katzenellenbogen, J. A. (2001) *J. Med. Chem.* **44,** 4230–4251
48. Shiau, A. K., Barstad, D., Loria, P. M., Cheng, L., Kushner, P. J., Agard, D. A., and Greene, G. L. (1998) *Cell* **95,** 927–937
49. Smith, C. L., and O'Malley, B. W. (2004) *Endocr. Rev.* **25,** 45–71
50. Kraichely, D. M., Sun, J., Katzenellenbogen, J. A., and Katzenellenbogen, B. S. (2000) *Endocrinology* **141,** 3534–3545
51. Watkins, R. E., Wisely, G. B., Moore, L. B., Collins, J. L., Lambert, M. H., Williams, S. P., Willson, T. M., Kliewer, S. A., and Redinbo, M. R. (2001) *Science* **292,** 2329–2333
52. Rajan, S. S., Yang, X., Shuvalova, L., Collart, F., and Anderson, W. F. (2004) *Biochemistry* **43,** 15472–15479
53. Sun, J., Baudry, J., Katzenellenbogen, J. A., and Katzenellenbogen, B. S. (2003) *Mol. Endocrinol.* **17,** 247–258
54. Muthyala, R. S., Sheng, S., Carlson, K. E., Katzenellenbogen, B. S., and Katzenellenbogen, J. A. (2003) *J. Med. Chem.* **46,** 1589–1602
55. Sibley, R., Hatoum-Mokdad, H., Schoenleber, R., Musza, L., Stirtan, W., Marrero, D., Carley, W., Xiao, H., and Dumas, J. (2003) *Bioorg. Med. Chem. Lett.* **13,** 1919–1922
56. Muthyala, R. S., Carlson, K. E., and Katzenellenbogen, J. A. (2003) *Bioorg. Med. Chem. Lett.* **13,** 4485–4488
57. Zhou, H. B., Comninos, J. S., Stossi, F., Katzenellenbogen, B. S., and Katzenellenbogen, J. A. (2005) *J. Med. Chem.* **48,** 7261–7274

Identification of Ligands with Bicyclic Scaffolds Provides Insights into Mechanisms of Estrogen Receptor Subtype Selectivity

Robert W. Hsieh, Shyamala S. Rajan, Sanjay K. Sharma, Yuee Guo, Eugene R. DeSombre, Milan Mrksich and Geoffrey L. Greene

J. Biol. Chem. 2006, 281:17909-17919.
doi: 10.1074/jbc.M513684200 originally published online April 28, 2006
